14. B. S. Petukhov, A. F. Polyakov, and S. V. Rosnovskii, "New approach to calculating heat transfer with the heat carrier at supercritical pressures," Teplofiz. Vys. Temp., 14, No. 6, 1326-1329 (1976).
15. A. F. Polyakov, "Development of secondary free convection flows in forced turbulent flow in horizontal pipes," Zh. Prikl. Mekh. Tekh. Fiz., No. 5, 60-66 (1974).
16. B. S. Petukhov, A. F. Polyakov, and Yu. L. Shekhter, "Turbulent flow and heat transfer in a gravitational force field," Teplofiz. Vys. Temp., 16, No. 3, 624-639 (1978).

# TURBULENT FLOW IN A RECTANGULAR CAVITY IN THE WALL OF A TWO-DIMENSIONAL CHANNEL

Ya. I. Kabakov and A. I. Maiorova

UDC 532.517.4

Results are presented of a theoretical and experimental investigation of flow of a turbulent incompressible liquid over a rectangular cavity of relative depth 1-3.

Separated flows of liquid or gas associated with flow over a cavity in a solid wall are encountered in many engineering installations. Such flows have received extensive study, in regard to their external features. Reference [1] has reviewed the experimental investigations of flow of a thick boundary layer over a rectangular cavity in the wall of a wind tunnel. Reference [2] has experimentally studied supersonic gas flow over a cavity in the wall of a two-dimensional channel, with a relative cavity depth to width of from 0.35 to 1.0. Reference [3] has presented results of measurement of the velocity of flow of an imcompressible liquid in a square cavity of width equal to four channel heights, at an incident stream Reynolds number of $\sim 7.5 \cdot 10^3$. Below we present results of an experimental and theoretical investigation of turbulent flow of an incompressible liquid in rectangular cavities in the wall of a two-dimensional channel for a cavity width equal to the channel height, relative depths of from 1 to 3, and Reynolds numbers from $10^4$ to $3.5 \cdot 10^5$

1. The turbulent characteristics were measured on an experimental facility, in the form of a channel of square section with side H = 0.1 m, made of clear plastic. The total channel length was 3.5 m. At a distance of 2.5 m from the channel entrance there was a rectangular cavity of extent d = H = 0.1 m, and the depth was varied in the range 0.1-0.3 m. The air entered the experimental facility from the atmosphere through a smooth entrance section, and was drawn in by vacuum pumps. The air velocity on the channel axis was varied from $U_0$ = 17 to $U_0$ = 60 m/sec with the help of a slide valve located at a distance of 1 m downstream of the cavity. To measure the velocities and the intensity of turbulence we used a constant-temperature hot-wire anemometer with a frequency characteristic of 30 kHz.

The main bulk of the measurements was made in the central plane of the channel. To determine the nature of the flow, we made control measurements at various longitudinal sections of the cavity. In the test range of Reynolds number, a noticeable breakdown of the two-dimensional flow was observed at distances up to 0.1d from the end walls. Taking into account what was said above, one can consider the flow to be approximately two-dimensional.

2. The method of calculation used in this work is based on numerical integration of the full system of steady-state Reynolds equations [4] for two-dimensional flow of an incompressible fluid:

$$U\frac{\partial U}{\partial x}+V\frac{\partial U}{\partial y}=-\frac{\partial P}{\partial x}+\nu\left(\frac{\partial^2 U}{\partial x^2}+\frac{\partial^2 U}{\partial y^2}\right)-\frac{\partial \overline{u^2}}{\partial x}-\frac{\partial \overline{uv}}{\partial y},$$

$$U\frac{\partial V}{\partial x}+V\frac{\partial V}{\partial y}=-\frac{\partial P}{\partial y}+\nu\left(\frac{\partial^2 V}{\partial x^2}+\frac{\partial^2 V}{\partial y^2}\right)-\frac{\partial \overline{uv}}{\partial x}-\frac{\partial \overline{v^2}}{\partial y}, \quad (1)$$

$$\frac{\partial U}{\partial x}+\frac{\partial V}{\partial y}=0.$$

Translated from Inzhenerno-Fizicheskii Zhurnal, Vol. 46, No. 3, pp. 363-371, March, 1984. Original article submitted January 14, 1983.

 0022-0841/84/4603-0252$08.50 

Here the bar above denotes averaging. Equations (1) do not form a closed system, since they contain new unknowns, the Reynolds stresses. To close the system of equations of the turbulent motion, we use various models of turbulence, containing empirical quantities. In this paper we have used the two-parameter k–ε and k–w models [5] and the Boussinesq hypothesis that the components of the Reynolds stress tensor depend linearly on the rate-of-strain tensor of the mean motion:

$$-\overline{u^2} = -\frac{2}{3}k + 2\nu_T\frac{\partial U}{\partial x}, \quad -\overline{v^2} = -\frac{2}{3}k + 2\nu_T\frac{\partial V}{\partial y}, \tag{2}$$

$$-\overline{uv} = \nu_T\left(\frac{\partial U}{\partial y} + \frac{\partial V}{\partial x}\right), \quad \nu_T = \frac{k}{\sqrt{w}} = C_D\frac{k^2}{\varepsilon},$$

where $\nu_T$ is the coefficient of turbulent viscosity. It is well known that these models are not rigorously founded and have a number of defects, but have been validated in the calculation of a large number of flows. More complex methods of closing the Reynolds equations (1) were used mainly in calculating flows of boundary-layer type. In addition, clearly the difficulties in obtaining a solution increase with the complexity of the model. Therefore, at present the two-parameter model of turbulence will evidently suffice as a theoretical basis for the study of separated flows, at least until one obtains more accurate experimental data.

Eliminating the pressure from Eq. (1), we write the equations of motion in stream function and vorticity variables:

$$U = \frac{\partial\psi}{\partial y}, \quad V = -\frac{\partial\psi}{\partial x}, \quad \omega = \frac{\partial V}{\partial x} - \frac{\partial U}{\partial y}. \tag{3}$$

Finally, the system of governing equations is written in the form

$$\frac{\partial^2\psi}{\partial x^2} + \frac{\partial^2\psi}{\partial y^2} = -\omega,$$

$$\frac{\partial}{\partial x}\left(\frac{\partial\psi}{\partial y}\omega\right) - \frac{\partial}{\partial y}\left(\frac{\partial\psi}{\partial x}\omega\right) - \frac{\partial}{\partial x}\left[(\nu_T+\nu)\frac{\partial\omega}{\partial x}\right] - \frac{\partial}{\partial y}\left[(\nu_T+\nu)\frac{\partial\omega}{\partial y}\right] = S_\omega, \tag{4}$$

$$\frac{\partial}{\partial x}\left(\frac{\partial\psi}{\partial y}k\right) - \frac{\partial}{\partial y}\left(\frac{\partial\psi}{\partial x}k\right) - \frac{\partial}{\partial x}\left[\left(\frac{\nu_T}{\sigma_k}+\nu\right)\frac{\partial k}{\partial x}\right] - \frac{\partial}{\partial y}\left[\left(\frac{\nu_T}{\sigma_k}+\nu\right)\frac{\partial k}{\partial y}\right] = S_k,$$

$$\frac{\partial}{\partial x}\left(\frac{\partial\psi}{\partial y}\varepsilon\right) - \frac{\partial}{\partial y}\left(\frac{\partial\psi}{\partial x}\varepsilon\right) - \frac{\partial}{\partial x}\left[\left(\frac{\nu_T}{\sigma_\varepsilon}+\nu\right)\frac{\partial\varepsilon}{\partial x}\right] - \frac{\partial}{\partial y}\left[\left(\frac{\nu_T}{\sigma_\varepsilon}+\nu\right)\frac{\partial\varepsilon}{\partial y}\right] = S_\varepsilon$$

using the k–ε model.

For the k–w model the last of Eqs. (4) is replaced by the following:

$$\frac{\partial}{\partial x}\left(\frac{\partial\psi}{\partial y}w\right) - \frac{\partial}{\partial y}\left(\frac{\partial\psi}{\partial x}w\right) - \frac{\partial}{\partial x}\left[\left(\frac{\nu_T}{\sigma_w}+\nu\right)\frac{\partial w}{\partial x}\right] - \frac{\partial}{\partial y}\left[\left(\frac{\nu_T}{\sigma_w}+\nu\right)\frac{\partial w}{\partial y}\right] = S_w.$$

Here the S are the source terms of the transport equations:

$$S_\omega = \left(\frac{\partial^2\nu_T}{\partial x^2} - \frac{\partial^2\nu_T}{\partial y^2}\right)\left(\frac{\partial U}{\partial y} + \frac{\partial V}{\partial x}\right) + 2\frac{\partial^2\nu_T}{\partial x\partial y}\left(\frac{\partial V}{\partial y} - \frac{\partial U}{\partial x}\right) + \frac{\partial\nu_T}{\partial x}\frac{\partial\omega}{\partial x} + \frac{\partial\nu_T}{\partial y}\frac{\partial\omega}{\partial y},$$

$$S_k = \nu_T F_k - \varepsilon = \nu_T F_k - C_D k\sqrt{w}, \quad S_\varepsilon = C_{\varepsilon 1}\frac{\varepsilon}{k}\nu_T F_k - C_{\varepsilon 2}\frac{\varepsilon^2}{k},$$

$$S_w = C_{w1}\nu_T F_w - C_{w2}w^{\frac{3}{2}} + C_{w3}\frac{w}{k}\nu_T F_k, \quad F_w = \left(\frac{\partial\omega}{\partial x}\right)^2 + \left(\frac{\partial\omega}{\partial y}\right)^2,$$

$$F_k = 2\left(\frac{\partial U}{\partial x}\right)^2 + 2\left(\frac{\partial V}{\partial y}\right)^2 + \left(\frac{\partial U}{\partial y} + \frac{\partial V}{\partial y}\right)^2, \quad U = \frac{\partial\psi}{\partial y}, \quad V = -\frac{\partial\psi}{\partial x}.$$

The values of the model constants $C_D$, $\sigma_k$, $\sigma_\varepsilon$, $\sigma_w$, $C_{\varepsilon 1}$, $C_{\varepsilon 2}$, $C_{w1}$, $C_{w2}$, $C_{w3}$ were those recommended in [5].

As the boundary condition at the impermeable walls, we gave values of the stream function $\psi = \psi_C$. In principle, at the walls we must assign the natural slip conditions for the velocity, the equality to zero of value of k, and the condition for w or ε, which follows from their definition

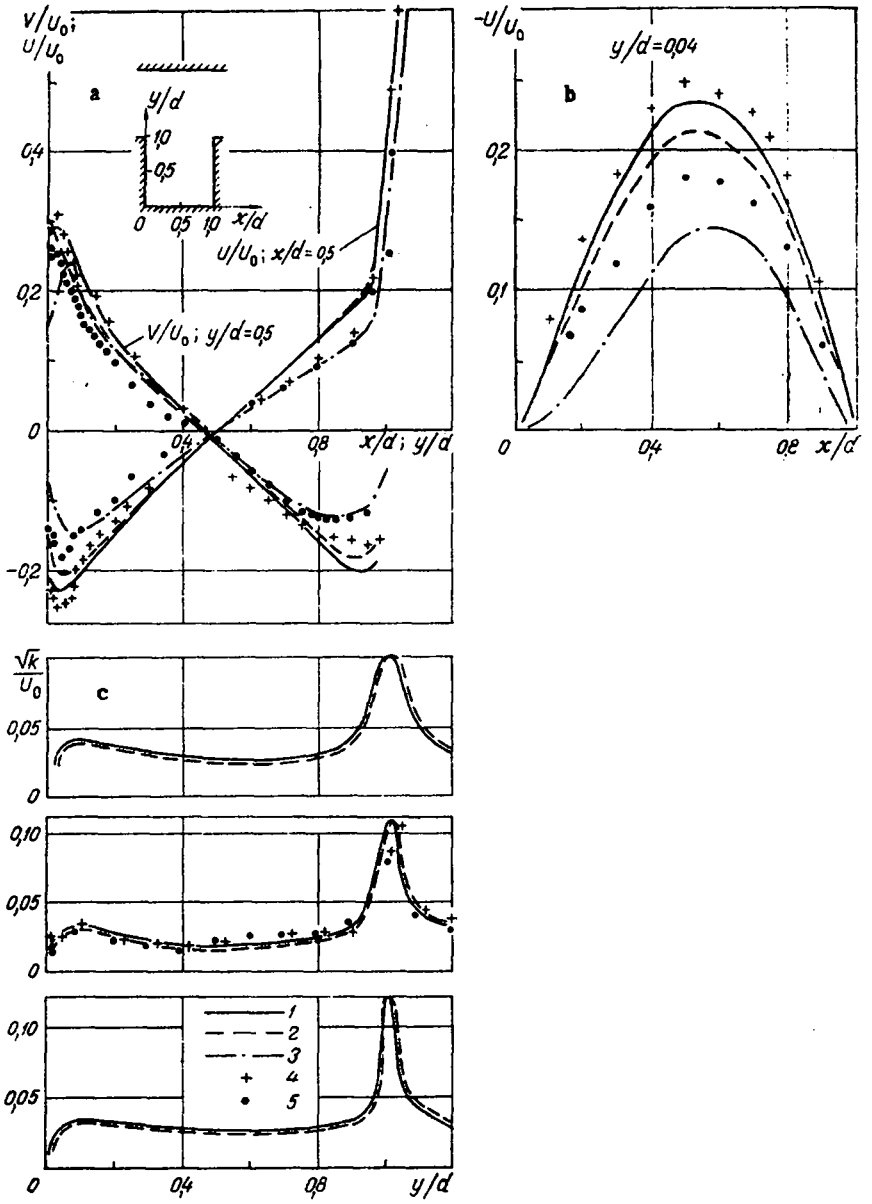


Fig. 1. Distribution of velocities in the mean sections (a) and along the floor (b) and of the intensity of turbulence (c) in a cavity with a relative depth of 1: 1-3) theory; 4, 5) experiment; 1, 4) Re = $3.5 \cdot 10^5$; 2, 5) $10^5$; 3) $10^4$. In Fig. 1c x/d = 0.79; 0.5 and 0.21 (from top to bottom).

$$\varepsilon = \nu \frac{\partial^2 k}{\partial n^2}, \quad w = \frac{\partial^2 k}{2\partial n^2}, \tag{5}$$

where n is the distance normal to the wall.

However, to accept these conditions requires changes in the turbulence model in the wall region, where the turbulent viscosity is close to the molecular value, and a considerable reduction of the mesh step size near the wall, and therefore the boundary conditions for all the quantities except $\psi$ are displaced by one step size into the flow, where we postulate that the universal "law of the wall" holds [4]:

$$\frac{U}{u^*} = \frac{1}{\varkappa} \ln \frac{u^* n}{\nu} + A, \quad k = \frac{u^{*2}}{\sqrt{C_D}}, \quad \varepsilon = \frac{u^{*3}}{\varkappa n}, \quad w = \frac{u^{*2}}{C_D \varkappa^2 n^2}, \tag{6}$$

$\varkappa$ = 0.41, A = 5.36, and u* is the dynamic viscosity. Integrating Eq. (6) with respect to n from 0 to $h_C$ (from the point C on the wall to the nearest point M on the normal to the wall), we obtain an approximate value of the liquid flow rate into a layer of height $h_C$:

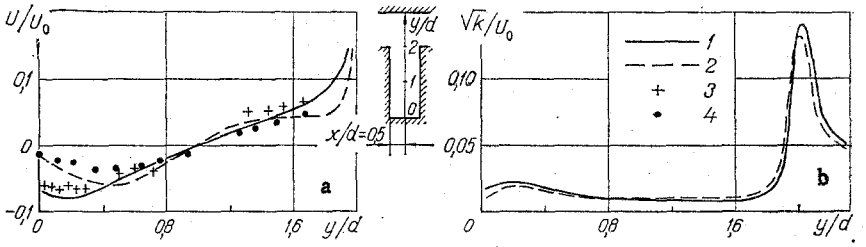


Fig. 2. Distribution of the longitudinal component of velocity (a) and of the intensity of turbulence (b) in the mean cross section of a cavity of relative depth 2: 1, 2) theory; 3, 4) experiment; 1, 3) Re = $3.5 \cdot 10^5$; 2, 4) $2.6 \cdot 10^4$.

$$|\psi_M - \psi_C| = u^* h_C \left( \frac{1}{\varkappa} \ln \frac{u^* h_C}{\nu} + A - \frac{1}{\varkappa} \right). \tag{7}$$

Hence, knowing the value of $\psi_M$ from Eq. (4), we can determine the value of u*. The vorticity at the point M is found by differentiating Eq. (6):

$$\omega_M = - \frac{u^*}{\varkappa n} \operatorname{sign} (\psi_M - \psi_C), \tag{8}$$

and $k_M$ and $\varepsilon_M(w_M)$ are determined from Eq. (5).

In the flow deceleration region where the "law of the wall" breaks down and the point of maximum generation of turbulent energy is at a distance from the wall, the quasilaminar conditions hold:

$$\psi = \psi_C, \ \omega_C = - \frac{1}{2} \omega_M - 3 \frac{\psi_M - \psi_C}{h_C^2}, \ k_C = 0, \ \frac{d\varepsilon_C}{dn} = \frac{dw_C}{dn} = 0. \tag{9}$$

At the channel entrance section we assigned the values of $\psi$, $\omega$, k, $\varepsilon$ corresponding to fully developed turbulent flow (with the "1/7" law). At the exit section we have the weak boundary conditions: the longitudinal derivatives of all the dependent variables are equal to zero. At the points closest to the corners, we have special boundary conditions as proposed in [6].

To obtain a finite-difference approximation the convective terms of Eq. (4) were replaced according to the hybrid scheme of [7], i.e., in the case where the convective terms do not exceed the diffusion terms we use central differences, and in the contrary case we use one-sided differences "counterflow." The diffusion terms were approximated to second-order accuracy. The merit of this scheme is its stability at high Reynolds numbers, but it can introduce diffusion additional to the physical "mesh" diffusion for large flow velocities and mesh step size, and therefore when using it one should monitor the results of the calculations, in terms of the experimental data. We note, however, that the velocities are small inside the cavity, and that the scheme has second-order accuracy almost everywhere. The system of algebraic equations obtained was solved by the Gauss–Seidel iteration method. The dynamic velocity u* was determined from Eq. (7). The calculations were done on the BÉSM-6 computer. A nonuniform finite-difference mesh was used, compressed in the regions with rapid change of flow characteristics: at the walls and in the layer where the circulating flow mixes with the external stream. The minimum mesh step size was 0.02d, and the maximum was 0.12d. A comparison of the results obtained with the k–w and k–$\varepsilon$ models showed that the difference between them fell within the experimental error, confirming the conclusion derived in [6] regarding the equivalence of the two-parameter models of turbulence in calculating separated flows.

3. Figures 1 and 2 show the flow characteristics in cavities with relative depth h/d = 1 and h/d = 2. As can be seen from Figs. 1 and 2 the computational model predicts the distribution of mean velocities and the energy of turbulence with satisfactory accuracy. The theory gives a Reynolds number dependence for the velocity distribution near the wall that is weaker than the experimental, possibly due to the use of the "law of the wall." On the other hand, some numerical divergence between the calculated and the experimental values of the velocities in the wall layers stems from the three-dimensionality of the flow due to friction of the vortex on the end walls of the channel, which leads to a small amount of disagreement in flow rates for the symmetric halves of the cavity section. With the turbulence

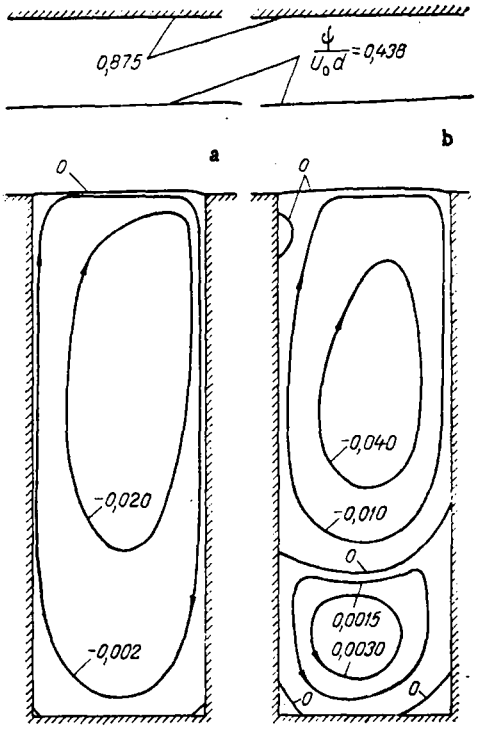


Fig. 3. Calculated picture of the flow in a cavity of depth 3: a) not allowing for streamline curvature; b) allowing for streamline curvature; Re = $3.5 \cdot 10^5$.

model both experiment and theory show that in cavities with relative depth 1 and 2 separated flow is generated in the form of a single stable vortex. It is known [1] that in a rectangular cavity of relative depth 2 in the wall of a wind tunnel (i.e., in a thick boundary layer) two vortices are formed, and therefore the pressure gradient has a stabilizing influence on the circulating flow, in spite of the fact that the friction at the walls is reduced, which one can determine by comparing the velocities at the walls with the data presented in [1]. The influence of the external pressure gradient also shows itself as a reduction of the maximum turbulent energy. The velocities at the trailing wall are greater than at the leading wall, i.e., the vortex is asymmetric. The intensity of turbulence (referenced to the maximum velocity at the entrance channel) remains almost constant within the cavity, and increases sharply in the layer of mixing of the circulating flow and the external stream. With an increased cavity depth the mean velocities at the walls and the intensity of turbulence in the separation region fall off in inverse proportion to the depth; the maximum intensity in the mixing layer remains constant.

For an increased incident stream Reynolds number the velocities at the wall increase. The distribution of energy of turbulence is practically independent of Reynolds number, as is shown by calculations in the Re range from $10^4$ to $10^6$.

4. A special feature of flow in cavities, observed experimentally, is well known [1]: the loss of stability of a vortex flow with increasing cavity depth, and disintegration of the vortex into two vortices rotating in opposite directions. The calculation of flow in a cavity of relative depth h/d = 3 according to the classical k–ε and k–w models of turbulence (Eqs. (4)) has shown that the models cannot describe this phenomenon (a single vortex is obtained in the calculation, see Fig. 3a). Calculation of a laminar flow according to the same finite-difference scheme gave a picture with two vortices, and therefore the cause of the error is an increase of the turbulent viscosity by the turbulence models because they do not account for the influence of streamline curvature on the spatial scale of turbulence. It is known [8, 9] that the relation between the turbulent stress tensor and the velocity field of the mean motion in the general case has the form

$$-\overline{u^2} = -\frac{2}{3}k + 2\nu_T^{11}\frac{\partial U}{\partial x} + 2\nu_T^{12}\frac{\partial U}{\partial y},$$

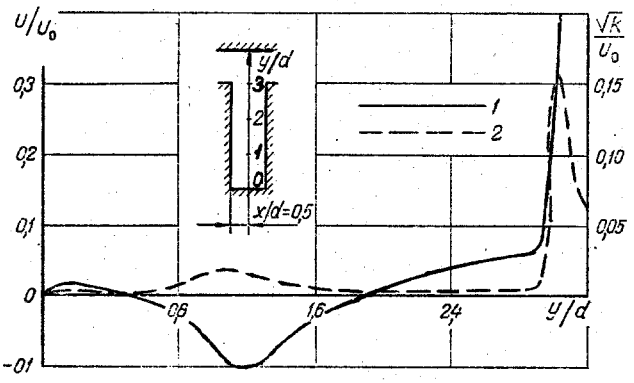


Fig. 4. Calculated distribution of the longitudinal component of velocity 1 and of the intensity of turbulence 2 in the mean cross section of a cavity of relative depth 3. Re = $3.5 \cdot 10^5$.

$$-\overline{v^2} = -\frac{2}{3}k + 2\nu_T^{21}\frac{\partial V}{\partial x} + 2\nu_T^{22}\frac{\partial V}{\partial y},$$

$$-\overline{uv} = \nu_T^{11}\frac{\partial V}{\partial x} + \nu_T^{12}\frac{\partial V}{\partial y} + \nu_T^{21}\frac{\partial U}{\partial x} + \nu_T^{22}\frac{\partial U}{\partial y}, \qquad (10)$$

where the $\nu_T^{ij}$ are components of the turbulent viscosity tensor. The conventional formulas of Eq. (2) are a simplified form of dependence (10). In two-dimensional turbulent flows, when the streamlines of the mean motion have curvature in the (x, y) plane, the structure of turbulence is altered by the centrifugal and Coriolis accelerations. This effect explains the improvement or the loss of stability of the flow field towards longitudinal perturbations. The rotation of the flow reduces the Reynolds shear stresses and the corresponding scales of turbulence, and also the turbulent energy, if the angular momentum of the motion increases with increasing distance from the center of rotation, and it increases them if the angular momentum decreases with increasing distance from the center of rotation. Here the tensors of the spatial scales of turbulence and of the turbulent viscosity may become appreciably anisotropic, which is not taken into account by Eq. (2) with an isotropic turbulent viscosity. A detailed discussion of this matter can be found in [10]. In [11], in an example of the calculation of the boundary layers around a body of revolution it was shown that in the first approximation one can account for curvature of the streamlines by adding to the dissipation term in the equation for ε or w an additional term depending on the derivative of the angular momentum with respect to the radius of curvature:

$$S_{\varepsilon 1} = S_\varepsilon + C_C \mathrm{Ri}\frac{\varepsilon^2}{k}C_{\varepsilon 2} = C_{\varepsilon 1}\frac{\varepsilon}{k}\nu_T F_k - C_{\varepsilon 2}(1 - C_C\mathrm{Ri})\frac{\varepsilon^2}{k},$$

$$S_{w1} = S_w + C_{w2}w^{\frac{3}{2}}C_C\mathrm{Ri} = C_{w1}\nu_T F_w + C_{w3}\nu_T F_k\frac{w}{k} - C_{w2}(1 - C_C\mathrm{Ri})w^{\frac{3}{2}}, \qquad (11)$$

$$C_C = 0{,}2,\ \mathrm{Ri} = \frac{k^2}{\varepsilon^2}\frac{V_\theta}{R^2}\frac{\partial}{\partial R}(RV_\theta) = \frac{1}{C_D^2 w}\frac{V_\theta}{R^2}\frac{\partial}{\partial R}(RV_\theta).$$

Here R is the distance to the center of rotation and $V_\theta$ is the rotational component of the velocity. As can easily be seen, for two-dimensional flow $V_\theta$ is the total velocity; R is the radius of curvature of the streamline:

$$\frac{1}{R} = \left|U^2\frac{\partial V}{\partial x} - V^2\frac{\partial U}{\partial y} + UV\left(\frac{\partial V}{\partial y} - \frac{\partial U}{\partial x}\right)\right| \Big/ (U^2 + V^2)^{3/2}. \qquad (12)$$

For cavities of depth d and 2d the calculation of the additional term led to some numerical change in the results, but this change, however, fell within the experimental error. For a cavity of depth 3d a very simple calculation of the curvature of the streamlines led to a qualitative change of the results of the calculations on both models, and gave a flow picture with two vortices (Fig. 3b).

The calculated profiles of velocity and intensity of turbulence are shown in Fig. 4, from which one can see that the velocity at the bottom of the cavity falls sharply, but the intensity of turbulence in this case does not remain constant in the separated flow region, and increases in the zone of interaction of the two vortices. We also verified a modification of the model, proposed in [12]:

$$S_{\varepsilon 2} = S_\varepsilon + C_{\varepsilon 1} C_{C_1} \mathrm{Ri}_1 \frac{\varepsilon}{k} \nu_T F_k, \tag{13}$$

$$S_{w2} = S_w + C_{w3} C_{C_1} \mathrm{Ri}_1 \frac{w}{k} \nu_T F_k, \; C_{C_1} = 0.03,$$

$$\mathrm{Ri}_1 = \frac{k}{\varepsilon} \frac{1}{R} \frac{\partial}{\partial R} (RV_\theta) = \frac{1}{C_D \sqrt{w}} \frac{1}{R} \frac{\partial}{\partial R} (RV_\theta),$$

but it did not have an appreciable influence on the results of the calculation. Thus, the modification of Eq. (11) gives a better description of the influence of streamline curvature on the structure of the turbulence.

We note that the corrections of Eqs. (11) and (13) are purely empirical. For a method of computing turbulent flows to have great universality, one must reject the conception of an isotropic turbulent viscosity and use relations of the type of Eq. (10). In our case, however, we are restrained from using more complex models by the absence of detailed experimental data on the characteristics of the flow in cavities of great depth.

## NOTATION

x, y, Cartesian coordinates; U, V and u, v, average and fluctuating velocity components; P, mean static pressure; H, channel height; d, cavity width; h, cavity depth; $U_0$, maximum velocity in a channel of height H; $\nu$, kinematic viscosity; $\mathrm{Re} = U_0 H/\nu$, Reynolds number; k, energy of turbulence per unit volume; w, square of the characteristic frequency of the turbulent fluctuations; $\varepsilon$, rate of dissipation of the energy of turbulence; Ri, Richardson number.

## LITERATURE CITED


1. P. K. Chang, Separation of Flow, Pergamon (1970).
2. V. K. Shchukin, Yu. F. Gortyshev, N. M. Varfolomeev, and N. A. Nadyrov, "The influence of relative depth and Reynolds number on heat transfer in cavities washed by an incompressible gas," Izv. Vyssh. Uchebn. Zaved., Aviats. Tekh., No. 3, 96 (1980).
3. V. Ya. Bogatyrev, Yu. N. Dubnishchev, V. A. Mukhin, et al., "Experimental investigation of flow in a slot," Zh. Prikl. Mekh. Teor. Fiz., No. 2, 76 (1976).
4. J. O. Hinze, Turbulence, McGraw-Hill (1975).
5. B. E. Launder and D. B. Spalding, Mathematical Models of Turbulence, Academic Press, London (1972).
6. A. I. Maiorova and V. I. Yagodkin, "Method and results of calculations of flows in channels with a sudden expansion," TsIAM, Tr. No. 883 (1980).
7. D. B. Spalding, "A novel finite-difference formulation for differential expressions involving both first and second derivatives," Int. J. Num. Eng., No. 4, 551 (1972).
8. A. S. Monin and A. M. Yaglom, Statistical Fluid Mechanics, Vol. 1, MIT Press (1975).
9. N. I. Buleev, "A test of the use of a spatial model of turbulent transfer," Teplofiz. Vys. Temp., No. 2, 312 (1976).
10. P. Bradshaw (ed.), Turbulence [Russian translation], Mashinostroenie, Moscow (1980).
11. B. I. Sharma, "Computation of flow past a rotating cylinder with an energy dissipation model of turbulence," AIAA J., 15, No. 2, 271 (1974).
12. C. Ha and B. Lakshiharayna, "Prediction of two- and three-dimensional asymmetric turbulent wakes, including curvature and rotation effects," AIAA J., 18, No. 10, 196 (1980).